Molecular Vision 2021; 27:415-428 <http://www.molvis.org/molvis/v27/415>
Received 25 November 2019 | Accepted 29 June 2021 | Published 1 July 2021

Mechanism of human γD-crystallin protein aggregation in UV-C light

Mangesh Bawankar, Ashwani Kumar Thakur

Department of Biological Sciences and Bioengineering, Indian Institute of Technology Kanpur, India

Purpose: To characterize intermediate aggregate species on the aggregation pathway of γD-crystallin protein in ultraviolet (UV)-C light.
Methods: The kinetics of γD-crystallin protein aggregation was studied with reversed-phase high-performance liquid chromatography (RP-HPLC) sedimentation assay, ThT binding assay, and light scattering. We used analytical ultracentrifugation to recognize intermediate aggregate species and characterized them with Fourier transform infrared spectroscopy (FTIR). Quantification of free sulfhydryl groups in an ongoing aggregation reaction was achieved by using Ellman's assay.
Results: Negligible lag phase was found in the aggregation kinetic experiments of the γD-crystallin protein. Dimer, tetramer, octamer, and higher oligomer intermediates were formed on the aggregation pathway. The protein changes its conformation to form intermediate aggregate species. FTIR and trypsin digestion indicated structural differences between the protein monomer, intermediate aggregate species, and fibrils. Ellman's assay revealed that disulfide bonds were formed in the protein monomers and aggregates during the aggregation process.
Conclusions: This study showed that various intermediate and structurally different aggregate species are formed on the aggregation pathway of γD-crystallin protein in UV-C light.

Cataract, an eye disease, causes opacification of the eye lens and is the foremost cause of blindness throughout the world [1,2]. Aggregation of crystallin proteins, mainly beta or gamma crystallins, is the primary cause of cataract formation. Surgical replacement of cataract lens with an artificial lens is the only treatment available for this disease [3,4]. However, in underdeveloped and developing countries, due to population load, the low number of ophthalmologists and insufficient surgical infrastructure hinder treatment [4,5]. Like other protein aggregation diseases, understanding the fundamental mechanism of crystallin protein aggregation will help in designing therapeutic molecules to suppress cataract formation. This will provide an alternative approach for treatment or delay the need for surgery. Thus, to understand the aggregation process in detail, it is critical to study the aggregation of γD-crystallin, a major component of cataract.

Humans are exposed inadvertently to either one or more types of ultraviolet (UV) light (UV-A, UV-B, and UV-C). They are often associated with the formation of crystallin protein aggregates. Several modifications, such as deamidation [6,7], oxidation [8], glycosylation [9], racemization [10], and truncation [10,11], were found in crystallin proteins isolated from cataract lens tissue. It was suggested that these modifications have a significant role to play in the aggregation of γD-crystallin protein in cataract disease. Existing literature indicates that γD-crystallin proteins form aggregates when exposed to UV-B light [12], low pH [13], heating at 80 °C [14], and guanidinium hydrochloride [15]. Further, Fourier transform infrared spectroscopy (FTIR) of porcine lenses induced with cataract by UV-B light indicates the signature of the amyloid structure in the lenses [16]. Proteolysis study of the fibrils formed in the presence of UV-B light showed that the C-terminal domain (84–174) of γD-crystallin protein is responsible for forming the amyloid core of the fibril [12]. Similarly, UV-C light also induces aggregation of γD-crystallin protein in vitro [17]. Although the ozone layer absorbs most of the UV-C rays from the sun, people living at high altitudes might be exposed to these rays. Artificial UV-C light is also used in houses and industrial appliances, making people prone to UV-C light. Therefore, along with UV-B light, it is equally important to study the effect of UV-C light on the aggregation of γD-crystallin proteins. Proteins have a generic nature of aggregation by forming various intermediate species [18,19]. These intermediates were structurally and morphologically different from the fibrillar structure formed at the end of the aggregation [18,19]. It is important to examine these intermediates, as many small molecules were reported to have a specific binding affinity for these intermediates species, potentially slowing the aggregation process [20,21].

Correspondence to: Ashwani Kumar Thakur, Department of Biological Sciences and Bioengineering, Indian Institute of Technology Kanpur, Kanpur – 208 016, UP, India; Phone: 05122594077; FAX: 05122594010; email: akthakur@iitk.ac.in

Interactions such as hydrogen bonding, hydrophobic interactions, electrostatic interactions, and disulfide bonds play a vital role in protein aggregation [22-24]. Among these interactions, the importance of disulfide bonds was reported in prion-related diseases, aggregates of tau proteins in Alzheimer disease, and cataract [25,26]. Aggregates isolated from cataract lens tissue were rich in disulfide bonds [27,28]. A high concentration of glutathione (GSH) maintains a reducing environment that prevents the formation of disulfide bonds of crystallin protein in lens cells. This keeps the lens away from opacity and provides a high transparency level for normal clear vision. However, as age increases, the GSH level drops in the lens fiber cells, leading to the formation of inter- and intra-disulfide bonds and loss of protein stability [29,30]. A recent study of γD-crystallin mutants stated that cys^{32} and cys^{41} are involved in disulfide bond formation when aggregated at 37 °C, pH 7 [31].

In this paper, we present the aggregation mechanism of γD-crystallin protein. We report the characterization of the intermediate species formed during the aggregation pathway of γD-crystallin under UV-C light. The quantification of free cysteines in monomers and aggregates is presented, suggesting the role of disulfide bonds in the aggregation.

METHOD

Materials and chemicals: Isopropyl β-D-1-thiogalactopyranoside (IPTG), TFA (trifluoroacetic acid (TFA), and Ellman's reagent [5,5′-dithiobis-(2-nitrobenzoic acid)] were purchased from Sisco Research Laboratories (Mumbai, India). Sodium chloride, monobasic sodium phosphate, sodium dibasic phosphate, and acetonitrile were purchased from Merck (Mumbai, India). ThT, 8-anilino-1-naphthalene-sulfonic acid (ANS), and trypsin were purchased from Sigma-Aldrich (Mumbai, India). Luria-Bertani (LB) broth and dialysis bags were purchased from Hi-media (Mumbai, India).

Protein purification: Plasmids containing a human γD crystallin gene were received as gifts from Prof. Martin Zanni (Department of Chemistry, University of Wisconsin-Madison, WI). The gene was cloned in pET-16b expression vector [32,33]. For protein expression, the recombinant plasmid was transformed in the BL21DE3 (pLys) bacterial strain. The recombinant bacteria were streaked on an LB-agar-ampicillin plate and incubated overnight at 37 °C. Next, a single colony from the plate was cultured in 10 ml LB-amp broth at 37 °C and 175 rpm overnight. This culture was added in 1 liter LB amp broth and incubated until 0.6 optical density (OD) was reached at 37 °C and 175 rpm. The culture was then induced with isopropyl β-D-1-thiogalactopyranoside (IPTG) and incubated further for 4 h. The cells were pelleted with centrifugation at 3,470 rcf, 4 °C for 15 min (Sorvall Lynx 6000, Thermo Scientific) and resuspended in binding buffer (20 mM phosphate buffer, 100 mM NaCl, 0.01% sodium azide, 10 mM imidazole, pH 7). The resuspended cells were lysed with probe sonication (repeated cycle of 20 s on, 40 s off for 30 min). The soluble proteins were separated from the cell debris by collecting the supernatant after centrifugation at 10,400 rcf at 4 °C for 30 min (Sorvall Lynx 6000, Thermo Scientific). The supernatant was applied to Ni-NTA (5 ml; Qiagen, Hilden, Germany) column followed by linear gradient elution with elution buffer (20 mM phosphate buffer, 100 mM NaCl, 0.01% sodium azide, and 500 mM imidazole, pH 7). The protein was further purified with dialysis using a dialysis buffer (20 mM phosphate buffer, 100 mM NaCl, 2 mM EDTA, and 0.01% sodium azide, pH 7) for 12 h at room temperature, replacing with fresh buffer every 3 h. The purified protein was then centrifuged at 139,600 rcf (Sorvall MTX 150, Thermo Scientific) at 4 °C before it was used for the experiments. The nucleotide sequence of the γD-crystallin gene was confirmed with plasmid sequencing (SciGenom, Kochi, India).

Determination of the concentration of the protein: Stock protein concentration was determined by taking O.D. at 280 nm using the extinction coefficient of 42,860 $M^{-1}cm^{-1}$. A standard curve was generated by injecting different concentrations of γD-crystallin protein in reversed-phase high-performance liquid chromatography (RP-HPLC). Then the area under the curve was calculated and plotted against different protein concentrations. The RP-HPLC-derived standard curve equation was used to determine the concentration of γD-crystallin for RP-HPLC sedimentation assay, light scattering, ThT binding assay, and atomic force microscopy (AFM). For analytical ultracentrifugation, the protein concentration was determined by taking O.D. at 280 nm using extinction coefficient 42,860 $M^{-1}cm^{-1}$ (calculated by using ExPASy at 280 nm). For other assays, the bicinchoninic acid (BCA) method was used to determine the concentration of γD-crystallin monomers, oligomers, and fibrils. For Ellman's assay, the aggregates collected at different time points of aggregation reaction were added in 8 M urea buffer (20 mM phosphate buffer + 100 mM NaCl, pH 7) and heated at 70 °C for 1 h until dissolved. Similarly, 8 M urea was added in the monomers at 0 h, the monomers were collected at different time points of the aggregation reaction, and the samples were heated at 70 °C for 1 h. The standard curve was prepared by using the BSA protein in the presence of 8 M urea, and the standard curve equation was used to determine the concentration of monomers and fibrils. The concentration of monomers, purified oligomers, and aggregates for tryptophan

fluorescence assay, ANS binding assay, and FTIR was also determined with the BCA method.

Spontaneous aggregation kinetics with RP-HPLC sedimentation assay, light scattering, and ThT binding assay: Aggregation of γD-crystallin protein was examined in a 4 ml quartz cuvette in a UV crosslinker chamber (Vilber Lourmat, Marne-la-Vallée, France) equipped with one UV-C lamp (8 W and 12 inches in length). The γD-crystallin protein at the concentration of 3 µM was incubated under UV-C light in dialysis buffer (20 mM phosphate buffer, 100 mM NaCl, 0.01% sodium azide, and 2 mM EDTA) at pH 7. Next, a 60 µl sample was collected at different time points and centrifuged at 139,600 rcf (Sorvall MTX 150, Thermo Scientific) for 30 min at 4 °C; then, 30 µl of supernatant was injected in the RP-HPLC (1260 Infinity system; Agilent Technologies, Santa Clara, CA) connected with a reverse phase C18 column (Eclipse plus, 3.5 µM, 4.6 × 100 mm, Agilent Technologies). The protein was eluted by increasing the linear gradient of acetonitrile (Solvent B) containing 0.05% TFA. Solvent A was composed of Milli-Q water, with 0.05% TFA. The absorbance of the protein was monitored at 215 nm. Then, from the area under the curve, percent monomers at the different time points were calculated [34]. Similarly, for light scattering and ThT binding assay, 150 µl of the sample was collected at each time point, and light scattering was monitored at 450 nm on the LS-55 fluorescence spectrometer (Perkin Elmer, Waltham, MA). Further, to know the presence of the amyloid structure, 25 µM ThT was added in the samples, which were used for light scattering. The ThT fluorescence intensity was measured at 450 nm excitation and 489 nm emission wavelengths. Emission and excitation slit widths were kept at 10 nm and 5 nm, respectively.

Analytical ultracentrifugation: Optima XL-I analytical ultracentrifuge (Beckman Inc., Indianapolis, IN) with an An-50Ti8 place rotor was used to perform sedimentation velocity experiments. γD-crystallin protein (40 µM) was incubated in 20 mM phosphate buffer and 100 mM NaCl, pH 7 under UV-C light for 1 h. Then, the samples were centrifuged at 19,000 rcf for 30 min to remove aggregated species, and supernatant was examined with analytical ultracentrifugation (AUC). For AUC, γD crystallin protein (25 µM) was centrifuged at 129,048 rcf and 20 °C by using a two-channel charcoal-filled centerpiece with Sapphire glass windows. The absorbance was monitored at 280 nm at each step, and an average of three scans was recorded. Using SEDFIT software (Bethesda, MD), a continuous distribution c(s) model was used to fit the data. The test Z values were below 20, and the root mean square deviation (RMSD) values of the fit data were in the range of 0.005 to 0.006. The partial specific volume value used was 0.71141, which was calculated from the primary protein sequence. The buffer density (ρ) and the buffer viscosity (η) were 1.00363 g/ml and 0.00906 poise, respectively. All these values were calculated by using SEDNTERP software.

Atomic force microscopy: Morphology of the intermediate aggregate species and fibrils was monitored under a multimode VIII Scanning Probe Microscope (Bruker, Billerica, MA) using the Peak Force-QNM mode. γD-crystallin protein (3 µM) was incubated under UV-C light. Then, a 3 µl sample was collected at different time points of the ongoing aggregation reaction and adsorbed on a freshly cleaved mica sheet. Further, the mica sheet containing the sample was washed three times with Milli-Q water and dried under a continuous nitrogen gas stream. The spherical particle diameter in the AFM images was measured in the x-axis direction using Nanoscope analysis software (Billerica, MA). That can give the exact size of a single sphere compared to the y- or z-axis [35,36]. The diameter of at least 60 particles was measured, and the average diameter of each time point was reported.

Purification of oligomers: γD-crystallin protein at 3 µM was incubated under UV-C light for 1 h to form oligomers. Then, the reaction mixture was centrifuged at 19,000 rcf for 20 min at 25 °C (Eppendorf 5417R). The pellet was washed three times with dialysis buffer (20 mM phosphate buffer, 100 mM NaCl, 0.01% sodium azide, and 2 mM EDTA, pH 7). Twenty milliliters of reaction mixture gives about 0.5 µM of oligomer species.

ANS binding assay, tryptophan fluorescence assay, and trypsin digestion: ANS dye at 35 µM was incubated with γD-crystallin monomers, oligomers, and fibrils in the dark for 10 min. Next, emission was monitored on the LS-55 spectrofluorometer (Perkin Elmer) instrument from wavelength 400−700 nm by using an excitation wavelength at 380 nm. Tryptophan fluorescence of γD-crystallin monomers, oligomers, and fibrils was also monitored on the same spectrofluorometer instrument. The concentration of monomers, oligomers, and fibrils was kept at 2.75 µM for the ANS and tryptophan assays. Tryptophan was excited at wavelength 295 nm, and emission was monitored from 310−390 nm. Excitation and emission slit width in both experiments was kept at 10 nm. The volume of reaction mixture used for each assay was 150 µl. For trypsin digestion, monomers, oligomers, and fibrils were incubated with trypsin (protein to trypsin ratio 10:1) for 16 h. Then, the samples (150 µl) were centrifuged at 2,900 rcf for 8 min, and the (90 µl) supernatant was injected in RP-HPLC (Agilent Technologies 1260 Infinity system) connected with the reverse phase C18 column (Eclipse plus, 3.5 µM, 4.6 × 100 mm, Agilent Technologies). The

concentrations of oligomers and fibrils were 0.5 µM, and that of trypsin was 0.05 µM; the concentrations of monomers and trypsin were 2 µM and 0.2 µM, respectively. RP-HPLC chromatograms were monitored at 215 nm.

Fourier transform infrared spectroscopy: The Bruker Tensor 27 FTIR instrument was used to record the spectra. With continuous nitrogen gas purging, 30 µl of γD-crystallin monomers, oligomers, and fibrils in 20 mM phosphate buffer containing 100 mM NaCl, 0.01% sodium azide, and 2 mM EDTA at pH 7 was loaded on a BIOATR II cell equipped with an mercury-cadmium-telluride (MCT) detector. The concentration of each species was 5 µM. At a resolution of 4 cm^{-1}, 120 scans were recorded to get a good S/N ratio. FTIR analysis was performed with OPUS software version 7.2. Using the rubber band correction method, baseline correction was performed (1,600 cm^{-1} to 1,700 cm^{-1}); 64 points were used. Next, the second derivative was calculated by using nine smoothening points. Using the Lavenberg Marquardt method, deconvolution of the original absorbance spectra was conducted from wavenumber 1,600 cm^{-1} to 1,700 cm^{-1}. The peak width was set at ten, and all wavenumbers corresponding to various secondary structures obtained from secondary derivative spectra were set to the maxima of the original absorbance spectra. For quantification, the integral value corresponding to each wavenumber was divided by the sum integral value of all wavenumbers to get a percent of secondary structures.

Ellman's assay: γD-crystallin protein at 25 µM was incubated under UV-C light. About 150 µl of the sample was collected at different time points and centrifuged at 19,000 rcf for 30 min. The supernatant containing protein monomers and the pellet containing aggregates were incubated separately with Ellman's reagent (1.28 mM) in the dark for 40 min. Ten micromolar concentrations of monomers and aggregates were taken at each time point. The volume of monomers and aggregates was 100 µl. Then, the yellow color intensity developed due to Ellman's reagent reaction with free sulfhydryl groups was measured on a plate reader at 412 nm [37]. A standard curve was generated using different concentrations of amino acid cysteine and used to quantify free sulfhydryl groups.

RESULTS

Aggregation kinetics of γD-crystallin protein: Aggregation kinetics was monitored with RP-HPLC sedimentation assay, light scattering, and ThT binding assay. RP-HPLC sedimentation assay is a sensitive and reliable technique for examining different phases of protein aggregation [34,38,39]. ThT dye is used to detect the amyloid feature of protein aggregates [40]. RP-HPLC data showed a decrease in percent monomer and increased aggregation with time (Figure 1, blue line). In contrast, light scattering (Figure 1, red line) and ThT binding (Figure 1, black line) increased as the aggregation progressed. Binding of ThT showed the presence of an amyloid-like structure in the aggregates. However, negligible ThT binding was observed during the initial time points of the aggregation kinetics in the ThT binding assays (Figure 1, inset), while the increase in light scattering and decrease in monomers were observed from the initial time points of the aggregation reaction. (Figure 1, inset, red). Thus, these initial aggregates might be different from the aggregates formed in the later stages and could be intermediate species during the aggregation pathway of γD-crystallin protein. To understand more details about these initial aggregates, analytical ultracentrifugation was performed.

Characterization of initial aggregate species: A sedimentation velocity (SV) experiment was performed to know heterogeneity, i.e., the presence of various aggregate species having different sizes in the reaction mixture [41,42]. Along with monomers, the presence of dimer, tetramer, octamer, and higher oligomer intermediates was observed (Table 1, Figure 2C,D). The abundance of dimers, tetramers, octamers, and higher oligomers was 6%, 4%, 5%, and 2%, respectively (Table 1). These values represent the significant amount of intermediate species present in the samples treated with UV-C for 1 h when compared with the abundance values of various species present without UV-C treatment (Table 1, Figure 2A,B). The molecular weights obtained from AUC may differ from the protein's actual molecular weight. This may be due to slight variation in the shapes of the protein monomers and intermediate aggregate species, while mathematical equations used in the analysis of the AUC data are based on the spherical shape of protein molecules [43-47].

Formation of oligomers on the aggregation pathway: The sedimentation velocity experiment indicated the presence of various intermediate species on the aggregation pathway of γD-crystallin protein under UV-C light. AFM was performed to know the morphology and sizes of these species. γD-crystallin protein at 3 µM was incubated under UV-C light, and samples were collected at different time points and examined under AFM (Figure 3). Spherical oligomers were observed until 1 h of the aggregation reaction. Further, quantification analysis showed an increase in size from monomers with 6±3 nm (n = 60) diameter at 0 h to 19±10 nm (n = 60) diameter after 0.6 h and then 63±18 nm (n = 60) diameter at 1 h (Figure 3). Next, at 3 h, higher aggregates were observed, which might have appeared due to the association of oligomers formed in the initial stages of aggregation reaction. AFM showed that the crystallin fibrils were formed after

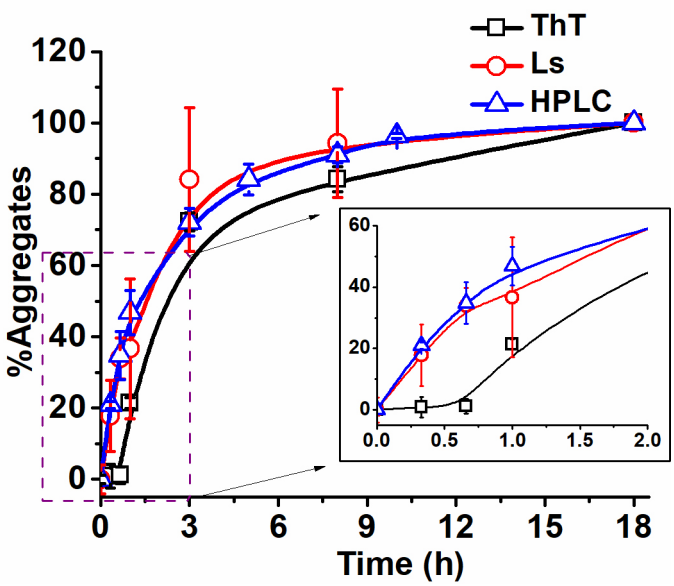

Figure 1. Aggregation kinetics of γD-crystallin under UV-C light. Reversed-phase high-performance liquid chromatography (RP-HPLC) sedimentation assay (blue), light scattering (red), and ThT binding (black) of γD-crystallin protein (3 µM) under ultraviolet (UV)-C light. Inset shows the aggregation reaction up to 2 h. In case of the RP-HPLC sedimentation assay, % monomers were converted to % aggregates, while the intensity values of light scattering and ThT binding assay are normalized considering intensity value at 18 h as 100%. n = 3 (n represents the number of times an experiment was repeated).

8 h. For oligomer characterization, we purified oligomers formed at 1 h and used them for the protein conformational examination and FTIR.

Conformation of γD-crystallin protein in oligomers and fibrils: AFM showed the presence of morphologically different species on the aggregation pathway of γD-crystallin protein under UV-C light. ThT binding was negligible to the initial aggregates. Therefore, it was hypothesized that there might be a change in the conformation of γD-crystallin protein in these morphologically different species (The Assembly of Protein Oligomers) [48,50]. Intrinsic tryptophan fluorescence, ANS binding, and trypsin digestion were performed to recognize changes in the state of γD-crystallin in monomers, oligomers, and fibrils. The tryptophan fluorescence intensity

Table 1. Molecular weights (kDa) and abundance of intermediate species present in the aggregation reaction of γD-crystallin.

Peak number	Protein species	Molecular weights	Abundance
Without UV−C			
1	Monomer	22.96±0.14	97.91±0.04
2	Tetramer	90.69±6.20	0.92±0.47
3	Oligomer	360.31	0.28
4	Oligomer	601.53±32.89	0.23±0.15
5	Oligomer	1044.61±54.03	0.11±0.10
After UV−C treatment for 1 h			
1	Monomer	23.01±0.31	79.44±11.89
2	Dimer	52.36±2.72	6.43±0.72
3	Tetramer	107.8±7.89	4.09±3.13
4	Octamer	196.31±5.64	4.99±1.31
5	Oligomer	450.63±57.38	1.15±0.11
6	Oligomer	861.52±19.67	0.42±0.35
7	Oligomer	1112.9±56.56	0.50±0.54

Note: Peak numbers correspond to Figure 2B,D. Experiment was repeated three times.

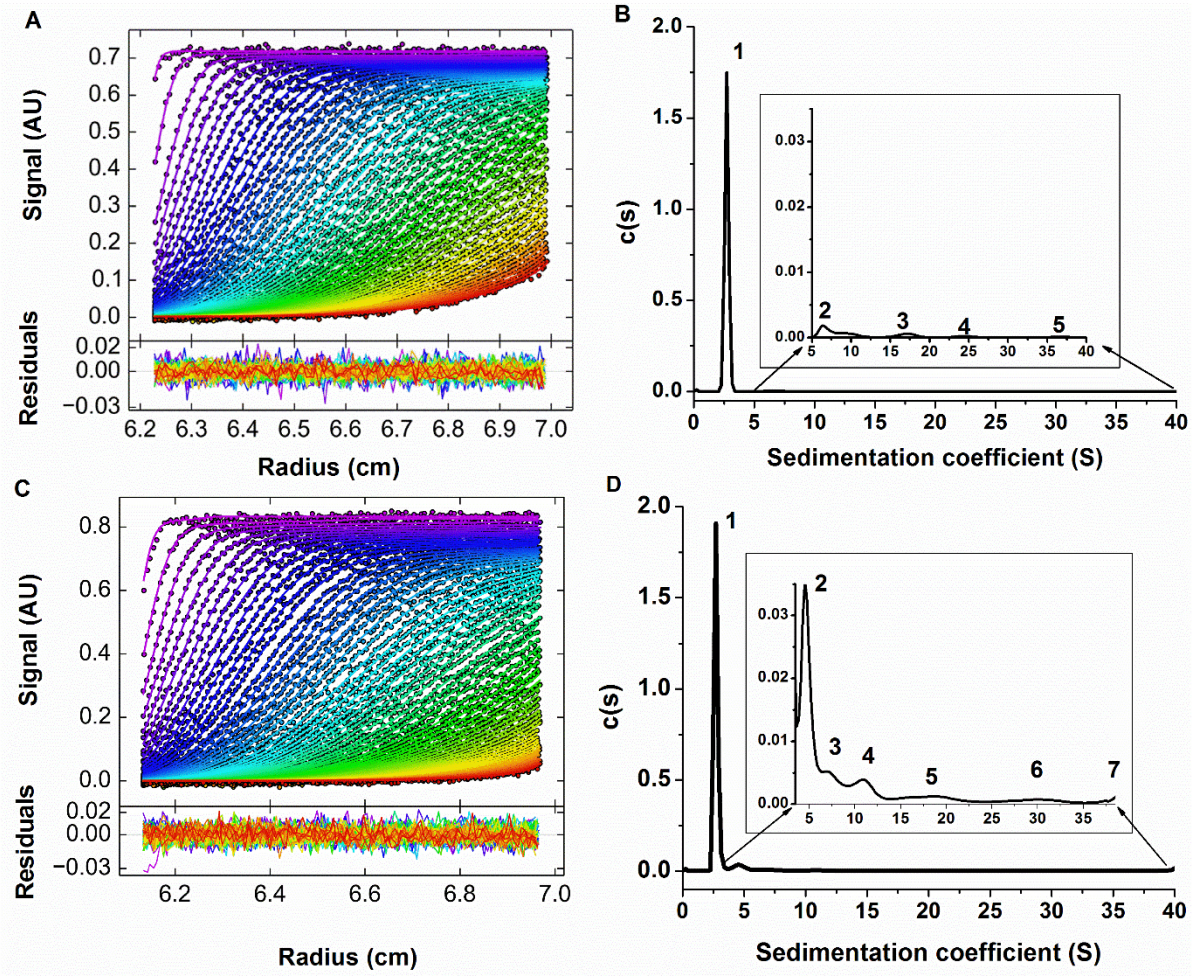

Figure 2. AUC of intermediate species of γD-crystallin aggregates formed under UV-C light. Raw sedimentation velocity centrifugation data of γD-crystallin protein without ultraviolet (UV)-C light (**A**) and after 1 h incubation under UV-C light (**C**). Molecular weight distribution of soluble species without UV-C light (**B**) and after 1 h incubation under UV-C light (**D**).

of the γD-crystallin monomers, oligomers, and fibrils was examined. As shown in Figure 4A, a shift in the λ_{max} was observed in the oligomers (348±0.57 nm, n = 3) and fibrils (353±1.00 nm, n = 3) when compared with the monomers (339±0.57 nm, n = 3). This shift might be due to a change in the tryptophan environment as a result of the unfolding of γD-crystallin protein during the formation of oligomers and fibrils [51]. ANS dye binds to exposed hydrophobic patches of unfolded protein and increases fluorescence intensity with a blue shift [51]. As shown in Figure 4B, a shift in the λ_{max} was observed from 532±0.60 nm (n=3) in monomers to 497±2.00 nm (n = 3) in oligomers and 500±0.60 nm (n = 3) in fibrils. Moreover, after binding of the dye to oligomers and fibrils, fluorescence intensity was increased compared to that of γD-crystallin monomers. This represents the exposure of hydrophobic amino acids of γD-crystallin protein in oligomers and fibrils. Another assay to identify the changes in the conformation of the protein in oligomers and fibrils is the treatment with sequence-specific proteases. If the protein conformation changes, then there could be a variation in the digestion pattern of the monomers, oligomers, and fibrils. Three RP-HPLC peaks were observed after trypsin digestion of γD-crystallin monomers, while nine peaks were observed after oligomer digestion, and no peaks were observed when fibrils were digested (Appendix 1). These results show that conformation and exposure of γD-crystallin protein to trypsin for cleavage are different in monomers, oligomers, and fibrils.

Secondary structure of γD-crystallin monomers, oligomers, and fibrils: FTIR was conducted to know the secondary structural changes in oligomers and fibrils with respect to monomers. Quantitative analysis revealed that the secondary structures of the oligomers were different from that of the fibrils and monomers (Table 2, Figure 5). Oligomers were

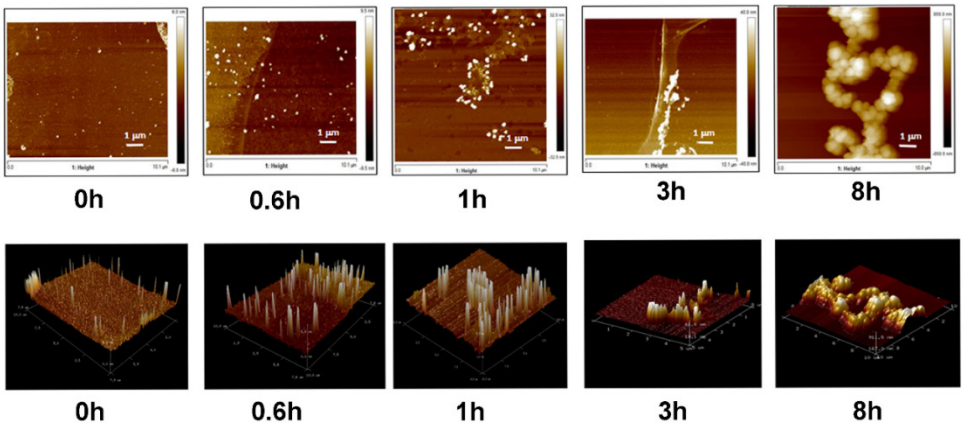

Figure 3. AFM images taken at different time points of the ongoing aggregation reaction of γD-crystallin in UV-C light. The upper panel shows a two-dimensional (2D) image of the samples collected from the ongoing aggregation reaction. The lower panel represents a three-dimensional (3D) view of the samples at the corresponding time point. The height of the samples is represented by the color bar present on the right side of the upper panel. Atomic force microscopy (AFM) images represent monomers, oligomers, and beaded fibrils. Scale bar = 1 µm.

found to be rich in random coil structure, while the percentage of α-helix was comparable to that of the fibrils. Further, oligomers were found to contain less β-turn than the fibrils.

Implications of disulfide bonds in the aggregation of γD-crystallin protein: The role of disulfide bonds in the aggregation of γD-crystallin protein under UV-C light has been reported in the literature [27,28]. The free sulfhydryl content was quantified by using Ellman's reagent. This reagent interacts with free sulfhydryl (−SH) groups and gives a yellow color [37]. The decrease in free sulfhydryl content was observed with the aggregates collected at different time points (Figure 6). The decrease in the free sulfhydryl groups was also observed in the supernatant containing protein monomers and other soluble aggregate species at different time points (Figure 6). The data suggest that disulfide bond formation upon UV-C exposure may be one of the drivers of γD-crystallin protein aggregation.

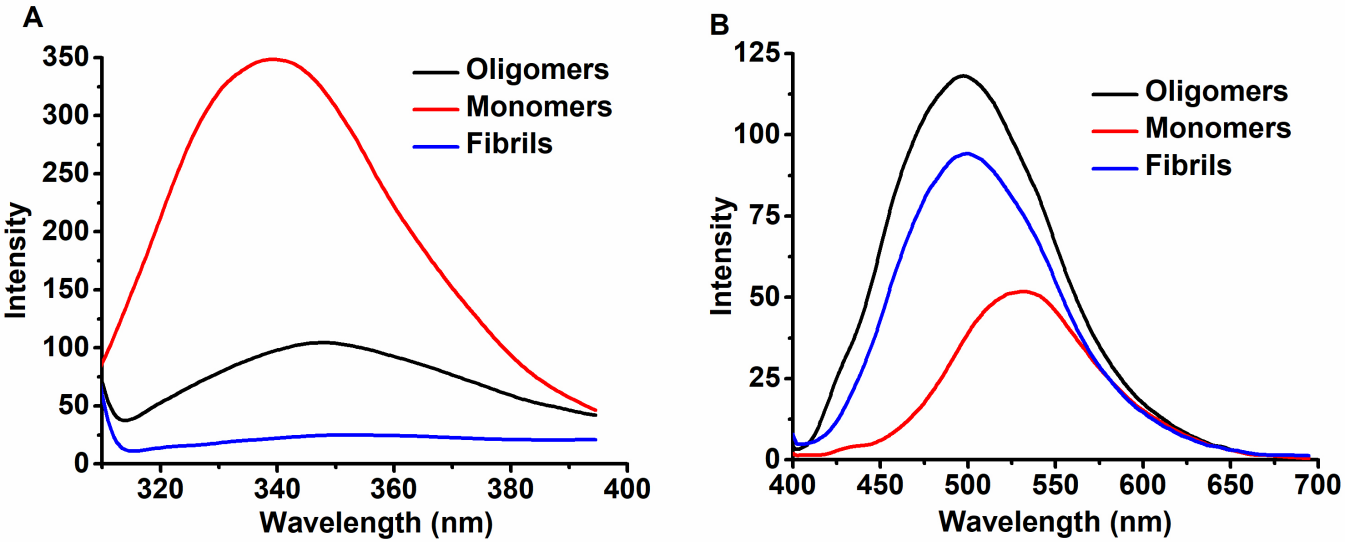

Figure 4. Protein conformational change study of monomers, oligomers, and fibrils. **A**: Tryptophan fluorescence assay. **B**: 8-anilino-1-naphthalene-sulfonic acid (ANS) binding assay of monomers, oligomers, and fibrils. The concentration of monomers, oligomers, and fibrils was 2.75 µM in both experiments. n = 3 (n represents number of times an experiment was repeated).

DISCUSSION

In the present work, we characterized intermediate aggregate species formed on the aggregation pathway of human γD crystallin protein under UV-C light. The results indicate that γD crystallin protein forms dimer, tetramer, octamer, and higher oligomer intermediates. Protein conformation and FTIR showed that the human γD crystallin protein undergoes unfolding to form intermediate aggregate species rich in a random coil structure.

Kinetic assays showed a negligible lag phase in the aggregation kinetics under UV-C light. The lag phase represents the time required for nuclei formation, which grows to reach an aggregate concentration that is readily detected [52]. The presence of a lag phase was reported in aggregation kinetics of polyglutamine peptides [39] and insulin [53]. In contrast, no significant lag phase was reported in human γD-crystallin protein under UV-B light [12], N-terminus huntingtin protein fragment [54], and IAPP [55] aggregation. We referred to aggregates or fibrils formed in UV-C light as amyloid-like because ThT binds to the fibrils and the presence of the β-sheet structure. Next, analytical ultracentrifugation experiments showed the presence of dimer, tetramer, octamer, and higher oligomer intermediates on the aggregation pathway. In the literature, sodium dodecyl sulfate polyacrylamide gel electrophoresis (SDS–PAGE) showed dimers as an intermediate species on the aggregation pathway of γD-crystallin under UV-C and UV-B light [17,56]. As per the literature, two monomer units were linked with a disulfide bond to form a dimer [17,56]. However, there could be another possibility of dimer and higher oligomer formation due to non-covalent interactions and without the formation of a disulfide bond. As in SDS–PAGE heating and SDS can break non-covalent interactions, this possibility was not ruled out in the previous study. In this study, various intermediate species in solution were examined without using any denaturing agent. AUC also showed an abundance of octamers (Table 1). Higher-order species on the aggregation pathway were reported to have less energy and thus, more stability than lower-order species

Table 2. Quantification of secondary structure content of the monomers, oligomers and fibrils.

Sr. no.	Secondary structure	Wavelength (cm^{-1})	Secondary structure (%)
	Monomers		
1	β-sheet (1630–1637 cm^{-1})	1637±0.16	56±0.56
2	β-turn (1662–1678 cm-1 and 1689–1699 cm-1)	1665±0.21	35±1.19
3	Antiparallel β-sheet (1679–1688 cm^{-1})	1685±0.10	9±0.64
	Oligomers		
1	Cross-β (1611–1630 cm^{-1})	1615±3.54	7±4
2	Cross-β (1611–1630 cm^{-1})	1628±1.18	15±11
3	Random coil (1637–1647 cm^{-1})	1642±2.49	31±6
4	α-helix (1647–1662 cm^{-1})	1661±0.81	34±2
5	Antiparallel β-sheet	1680±0.5	10±2
6	β-turn	1692±0.26	2±0.3
	Fibrils		
1	Cross-β	1614±0.71	3±0.35
2	β-sheet	1632±0.49	27±1.34
3	Random coil	1643±0.17	14±1.95
4	α-helix	1659±0.51	32±1.84
5	β-turn	1677±0.52	21±2.05
6	β-turn	1690±0.20	3±0.13

Note: Secondary structure assignment was done as per literature [63]. Experiment was repeated three times.

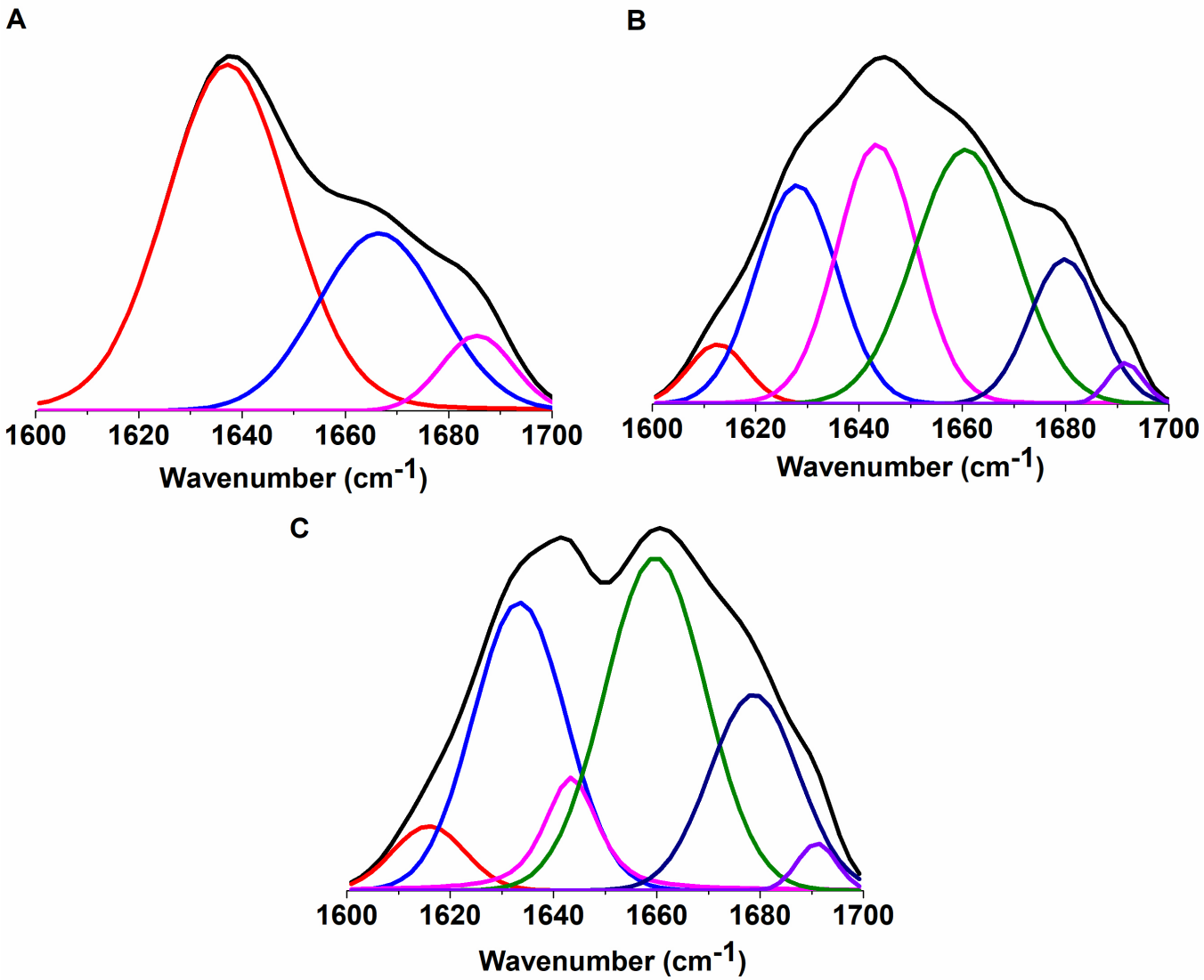

Figure 5. Fourier transform infrared spectroscopy (FTIR) of monomers, oligomers, and fibrils. Curve fit spectra of (**A**) monomers, (**B**) oligomers, and (**C**) fibrils. n = 3 (n represents number of times an experiment was repeated).

[57,58]. It was suggested that the formation of intermolecular interactions in higher-order species leads to more stability of these species over lower-order species [57,58].

In the amyloid protein aggregation pathway, initial aggregates species were reported to be oligomers, and to understand the aggregation mechanism of amyloid aggregation, it is essential to characterize them. Therefore, we characterized the oligomers formed after 1 h of aggregation reaction as shown with AFM because these oligomers are bigger than that at 0.6 h (Figure 3). This difference in size at two different time points helps in the isolation of these bigger species from the remaining monomers. Data obtained from the aggregation kinetics, AUC, and AFM can be used to propose an aggregation pathway under UV-C light. In the aggregation process, γD-crystallin monomers may form a dimer, and then two dimers or one dimer with two monomers may associate to form a tetramer (Figure 7). Next, an octamer would be formed by the association of two tetramers or two dimers with one tetramer; or the association of four monomers with one tetramer. Further, these octamers grow to form higher oligomer species by associations of these initial species (dimer, tetramer, and octamer) and the addition of monomers to form fibrils (Figure 7). Next, ANS fluorescence intensity was observed to be higher in the case of oligomers and fibrils than in monomers (Figure 4 B). Among oligomers and fibrils, more fluorescence intensity was found in oligomers. This might be due to the exposure of more hydrophobic residues to solvent in oligomers than

fibrils. Therefore, the ANS experiment suggested that in the presence of UV-C light, γD-crystallin monomers first change their conformation to form oligomers containing more hydrophobic patches (Figure 7, shown in red). These oligomers then undergo another conformational change, where less hydrophobic residues are exposed to form fibrils (Figure 7). Trypsin digestion also represents a change in protein conformation in oligomers. γD-crystallin has 21 arginines and one lysine residue in its primary sequence. Trypsin cleaves at the C-terminal end of arginine and lysine [59]. Therefore, theoretically, approximately 23 fragments should have been generated after trypsin digestion. However, considering all the known facts about trypsin digestion [59,60], 14 peptide fragments are expected to be generated after digestion (Appendix 2). In human γD-crystallin protein, all arginine and lysine residues are exposed to solvent Appendix 3 panel A); however, because of the structural constraint of γD-crystallin monomers, only three digested fragments were observed. The structural constraints of protein include (a) the location of lysine and arginine at active site positions may have reduced the binding due to steric hindrance, and (b) the presence of the cleavage sites on various secondary structures also leads to less cleavage [60]. Cleavage sites present within the rigid secondary structures (α-helix and β-sheet) are more resistant to proteolysis than those present on disordered flexible structures [60]. γD-crystallin protein structure contains 15 arginine residues on the α-helix and β-sheet, and six arginine and one lysine are present on the β-turn (Appendix 3 panel B,C). Approximately nine fragments were seen after the digestion of oligomers because of less structural constraint of γD-crystallin in oligomers than monomers Appendix 1). No digested peaks were observed after the digestion of fibrils. This might be due to the rigid structure of fibrils, thus providing structural constraints for protein digestion. Therefore, the proteolysis event depends on the specificity and the conformation of the target protein. Thus, it can be inferred that the conformation state of γD-crystallin protein and the secondary structure of monomers, oligomers, and fibrils are different. In literature, a similar proteolysis experiment was performed on lysozyme oligomers [61]. Similar to γD-crystallin oligomers, more proteolysis fragments were reported after digestion with oligomers than lysozyme monomers [61]. Therefore, it may be concluded that proteolysis results obtained for γD-crystallin oligomers match other amyloid protein oligomers reported in the literature. FTIR revealed that oligomers are rich in random coil structure (Table 2). This might be the reason for the increased number of digested fragments after trypsin digestion (Figure S1). Using Ellman's assay, we showed that disulfide bonds are formed in protein monomers during aggregation (Figure 6). The presence of urea during the estimation of the protein concentration might have some interference in the BCA method [62]. However, this error in determining the protein concentration will be similar in all

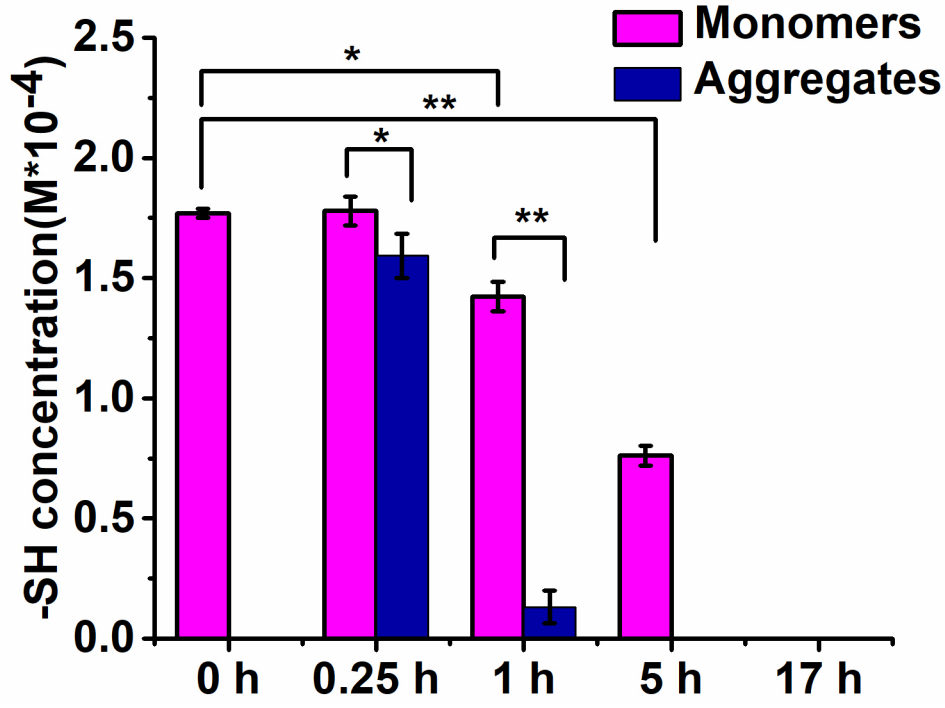

Figure 6. Ellman's assay to determine free sulfhydryl groups (-SH) groups in monomers and aggregates collected at different time points. n = 3 (n represents number of times an experiment was repeated), *p<0.05, **p<0.0001 (unpaired Student *t* test was used to determine the level of significance).

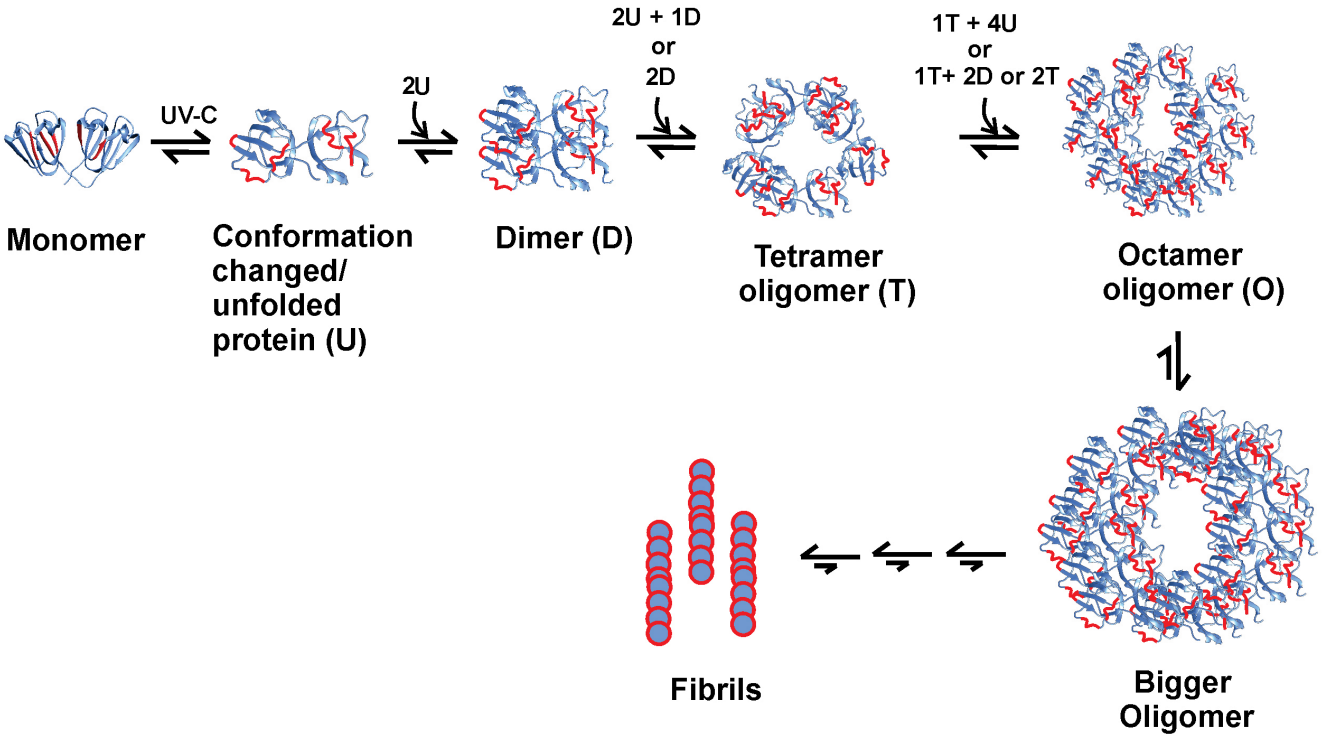

Figure 7. Proposed aggregation pathway for aggregation of γD-crystallin protein in UV-C light. Monomer PDB id is 1HK0; all other images are only for representative purposes. Red shows the hydrophobic patches in the protein.

samples, i.e., monomers and fibrils. Next, this error will be compensated when comparing each species at different time points of the aggregation reaction. Additionally, the role of disulfide bonds in the aggregation is known in the literature [27,28]. In the present study, we showed that disulfide bonds are formed in the γD-crystallin protein monomer of ongoing aggregation reaction.

We reported the presence of various intermediate aggregate species in UV-C light for the first time. The AUC showed that the aggregation starts with the formation of dimer, tetramer, octamer, and bigger oligomer intermediates (Figure 7). AFM confirmed the presence of spherical oligomers on the aggregation pathway. FTIR indicated these oligomers are abundant in random coil structure, which is easily digested by trypsin compared to monomers. This study opens up new avenues for research to understand the detailed aggregation mechanism and the aggregation hotspot of γD-crystallin in cataract formation.

APPENDIX 1. RP-HPLC CHROMATOGRAMS OBTAINED AFTER DIGESTION OF MONOMERS, OLIGOMERS AND FIBRILS WITH TRYPSIN.

To access the data, click or select the words "Appendix 1." (*Indicates peak of enzyme trypsin, in monomers (cyan), trypsin peak was not visible due to more peak area of the fragment obtained after digestion, at same R.T. of trypsin).

APPENDIX 2. POSSIBLE FRAGMENTS EXPECTED AFTER TRYPSIN DIGESTION.

To access the data, click or select the words "Appendix 2."

APPENDIX 3. REPRESENTATION OF ARGININE AND LYSINE ON THE CRYSTAL STRUCTURE OF γD-CRYSTALLIN PROTEIN.

To access the data, click or select the words "Appendix 3." (A) Mesh shows all the residues (arginine - red and lysine - cyan) in γD-crystallin protein are exposed to the solvent; (B) Fifteen arginine residues (red) are present on the α-helix and β-sheet; (C) Six arginine and one lysine residues are present on the β-turn (blue) (chimera, PDB ID 1HK0).

ACKNOWLEDGMENTS

We sincerely thank Prof. Martin Zanni (Department of Chemistry, University of Wisconsin Madison, USA) for providing clone of γD crystallin protein. We greatly appreciate Saravanan Matheshwaran (Department of Biologic Sciences and Bioengineering, Indian Institute of Technology Kanpur, India) for allowing us to use FPLC for protein purification. The usage of analytical ultracentrifugation facility of Institute of Microbial Technology (CSIR), Chandigarh, India is highly acknowledged. Mangesh Bawankar acknowledges Ministry of Human Resource Development and Indian Institute of Technology Kanpur, India for fellowship. Funding Source: Study supported by Indian Institute of Technology Kanpur grant IITKBSBE100293.

REFERENCES

1. Mariotti A, Pascolini D. Global estimates of visual impairment. Br J Ophthalmol 2012; 96:614-8. [PMID: 22133988].
2. Bourne RR, Stevens GA, White RA, Smith JL, Flaxman SR, Price H, Jonas JB, Keeffe J, Leasher J, Naidoo K. Causes of vision loss worldwide, 1990–2010: a systematic analysis. Lancet Glob Health 2013; 1:e339-49. [PMID: 25104599].
3. Lam D, Rao SK, Ratra V, Liu Y, Mitchell P, King J, Tassignon M-J, Jonas J, Pang CP, Chang DF. Cataract. Nat Rev Dis Primers 2015; 1:15014-[PMID: 27188414].
4. Moreau KL, King JA. Protein misfolding and aggregation in cataract disease and prospects for prevention. Trends Mol Med 2012; 18:273-82. [PMID: 22520268].
5. Haddad NMN, Sun JK, Abujaber S, Schlossman DK, Silva PS. Cataract surgery and its complications in diabetic patients. Semin Ophthalmol 2014; 29:329-37. [PMID: 25325858].
6. Hains PG, Truscott RJ. Age-dependent deamidation of lifelong proteins in the human lens. Invest Ophthalmol Vis Sci 2010; 51:3107-14. [PMID: 20053973].
7. Wilmarth P, Tanner S, Dasari S, Nagalla S, Riviere M, Bafna V, Pevzner P, David L. Age-related changes in human crystallins determined from comparative analysis of post-translational modifications in young and aged lens: does deamidation contribute to crystallin insolubility? J Proteome Res 2006; 5:2554-66. [PMID: 17022627].
8. Garner MH, Spector A. Selective oxidation of cysteine and methionine in normal and senile cataractous lenses. Proc Natl Acad Sci USA 1980; 77:1274-7. [PMID: 6929483].
9. Lee JH, Shin DH, Lupovitch A, Shi DX. Glycosylation of lens proteins in senile cataract and diabetes mellitus. Biochem Biophys Res Commun 1984; 123:888-93. [PMID: 6487331].
10. Lyons B, Jamie JF, Truscott RJ. Separate mechanisms for age-related truncation and racemisation of peptide-bound serine. Amino Acids 2014; 46:199-207. [PMID: 24306455].
11. Santhoshkumar P, Udupa P, Murugesan R, Sharma KK. Significance of interactions of low molecular weight crystallin fragments in lens aging and cataract formation. J Biol Chem 2008; 283:8477-85. [PMID: 18227073].
12. Moran SD, Zhang TO, Decatur SM, Zanni MT. Amyloid fiber formation in human γD-crystallin induced by UV–B photodamage. Biochemistry 2013; 52:6169-81. [PMID: 23957864].
13. Papanikolopoulou K, Mills-Henry I, Thol SL, Wang Y, Gross AAR, Kirschner DA, Decatur SM, King J. Formation of amyloid fibrils in vitro by human γD-crystallin and its isolated domains. Mol Vis 2008; 14:81-9. [PMID: 18253099].
14. Moran SD, Zhang TO, Zanni MT. An alternative structural isoform in amyloid-like aggregates formed from thermally denatured human γD-crystallin. Protein Sci 2014; 23:321-31. [PMID: 24415662].
15. Shanmugam PM, Barigali A, Kadaskar J, Borgohain S, Mishra DKC, Ramanjulu R, Minija CK. Effect of lanosterol on human cataract nucleus. Indian J Ophthalmol 2015; 63:888-90. [PMID: 26862091].
16. Zhang TO, Alperstein AM, Zanni MT. Amyloid β-Sheet Secondary Structure Identified in UV-Induced Cataracts of Porcine Lenses Using 2D IR Spectroscopy. J Mol Biol 2017; 429:1705-21. [PMID: 28454743].
17. Wang SSS, Wen W-S. Examining the influence of ultraviolet C irradiation on recombinant human γD-crystallin. Mol Vis 2010; 16:2777-90. [PMID: 21197112].
18. Bemporad F, Chiti F. Protein misfolded oligomers: experimental approaches, mechanism of formation, and structure-toxicity relationships. Chem Biol 2012; 19:315-27. [PMID: 22444587].
19. Sengupta I, Udgaonkar JB. Structural mechanisms of oligomer and amyloid fibril formation by the prion protein. Chem Commun 2018; 54:6230-42. [PMID: 29789820].
20. Bieschke J, Herbst M, Wiglenda T, Friedrich RP, Boeddrich A, Schiele F, Kleckers D, del Amo JML, Grüning BA, Wang Q. Small-molecule conversion of toxic oligomers to nontoxic β-sheet–rich amyloid fibrils. Nat Chem Biol 2012; 8:93-101. [PMID: 22101602].
21. Ladiwala ARA, Dordick JS, Tessier PM. Aromatic small molecules remodel toxic soluble oligomers of amyloid β through three independent pathways. J Biol Chem 2011; 286:3209-18. [PMID: 21098486].
22. Vogt G, Woell S, Argos P. Protein thermal stability, hydrogen bonds, and ion pairs. J Mol Biol 1997; 269:631-43. [PMID: 9217266].
23. Xiao L, Honig B. Electrostatic contributions to the stability of hyperthermophilic proteins. J Mol Biol 1999; 289:1435-44. [PMID: 10373377].
24. Betz SF. Disulfide bonds and the stability of globular proteins. Protein Sci 1993; 2:1551-8. [PMID: 8251931].
25. Mossuto MF. Disulfide bonding in neurodegenerative misfolding diseases. Int J Cell Biol 2013; xxx:318319-.
26. Yu N-T, DeNagel DC, Pruett PL, Kuck J. Disulfide bond formation in the eye lens. Proc Natl Acad Sci USA 1985; 82:7965-8. [PMID: 3865209].

27. Ozaki Y, Mizuno A, Itoh K, Iriyama K. Inter-and intramolecular disulfide bond formation and related structural changes in the lens proteins. A Raman spectroscopic study in vivo of lens aging. J Biol Chem 1987; 262:15545-51. [PMID: 3680210].

28. Ozaki Y, Mizuno A. Molecular aging of lens crystallins and the life expectancy of the animal. Age-related protein structural changes studied in situ by Raman spectroscopy. Biochimica et Biophysica Acta (BBA)- Protein Structure and Molecular Enzymology 1992; 1121:245-51. [PMID: 1627601].

29. Lou MF, Dickerson JE, Garadi R. The role of protein-thiol mixed disulfides in cataractogenesis. Exp Eye Res 1990; 50:819-26. [PMID: 2373174].

30. Lou MF, Xu G-T, Cui X-L. Further studies on the dynamic changes of glutathione and protein-thiol mixed disulfides in H2O2 induced cataract in rat lenses: distributions and effect of aging. Curr Eye Res 1995; 14:951-8. [PMID: 8549161].

31. Serebryany E, Woodard JC, Adkar BV, Shabab M, King JA, Shakhnovich EI. An internal disulfide locks a misfolded aggregation-prone intermediate in cataract-linked mutants of human γD-crystallin. J Biol Chem 2016; 291:19172-83. [PMID: 27417136].

32. Moran SD, Woys AM, Buchanan LE, Bixby E, Decatur SM, Zanni MT. Two-dimensional IR spectroscopy and segmental 13C labeling reveals the domain structure of human γD-crystallin amyloid fibrils. Proc Natl Acad Sci USA 2012; 109:3329-34. [PMID: 22328156].

33. Moran SD, Decatur SM, Zanni MT. Structural and sequence analysis of the human γD-crystallin amyloid fibril core using 2D IR spectroscopy, segmental 13C labeling, and mass spectrometry. J Am Chem Soc 2012; 134:18410-6. [PMID: 23082813].

34. O'Nuallain B, Thakur AK, Williams AD, Bhattacharyya AM, Chen S, Thiagarajan G, Wetzel R. Kinetics and Thermodynamics of Amyloid Assembly Using a High-Performance Liquid Chromatography–Based Sedimentation Assay. Methods Enzymol 2006; 413:34-74. [PMID: 17046390].

35. Adamcik J, Lara C, Usov I, Jeong JS, Ruggeri FS, Dietler G, Lashuel HA, Hamley IW, Mezzenga R. Measurement of intrinsic properties of amyloid fibrils by the peak force QNM method. Nanoscale 2012; 4:4426-9. [PMID: 22688679].

36. Mishra R, Thakur AK. Amyloid nanospheres from polyglutamine rich peptides: assemblage through an intermolecular salt bridge interaction. Org Biomol Chem 2015; 13:4155-9. [PMID: 25692827].

37. Riener CK, Kada G, Gruber HJ. Quick measurement of protein sulfhydryls with Ellman's reagent and with 4, 4′-dithiodipyridine. Anal Bioanal Chem 2002; 373:266-76. [PMID: 12110978].

38. Wetzel R. Physical chemistry of polyglutamine: Intriguing tales of a monotonous sequence. J Mol Biol 2012; 421:466-90. [PMID: 22306404].

39. Bhattacharyya AM, Thakur AK, Wetzel R. Polyglutamine aggregation nucleation:therm odynamics of a highly unfavorable protein folding reaction. Proc Natl Acad Sci USA 2005; 102:15400-5. [PMID: 16230628].

40. Biancalana M, Koide S. Molecular mechanism of thioflavin-T binding to amyloid fibrils. Biochim Biophys Acta 2010; 1804:1405-12. [PMID: 20399286].

41. Lelj-Garolla B, Mauk AG. Self-association of a Small Heat Shock Protein. J Mol Biol 2005; 345:631-42. [PMID: 15581903].

42. Lebowitz J, Lewis MS, Schuck P. Modern analytical ultracentrifugation in protein science: A tutorial review. Protein Sci 2002; 11:2067-79. [PMID: 12192063].

43. Cole JL, Lary JW. P Moody T, Laue TM. Analytical ultracentrifugation: sedimentation velocity and sedimentation equilibrium. Methods Cell Biol 2008; 84:143-79. [PMID: 17964931].

44. Schuck P. On the analysis of protein self-association by sedimentation velocity analytical ultracentrifugation. Anal Biochem 2003; 320:104-24. [PMID: 12895474].

45. Dam J, Velikovsky CA, Mariuzza RA, Urbanke C, Schuck P. Sedimentation velocity analysis of heterogeneous protein-protein interactions: Lamm equation modeling and sedimentation coefficient distributions c(s). Biophys J 2005; 89:619-34. [PMID: 15863475].

46. Reynolds JA, McCaslin DR. Determination of protein molecular weight in complexes with detergent without knowledge of binding. Methods Enzymol 1985; 117:41-53. [PMID: 2934606].

47. Stafford WF. Boundary analysis in sedimentation transport experiments: a procedure for obtaining sedimentation coefficient distributions using the time derivative of the concentration profile. Anal Biochem 1992; 203:295-01. [PMID: 1416025].

48. Okamoto K, Hiroshima M, Sako Y. Single-molecule fluorescence-based analysis of protein conformation, interaction, and oligomerization in cellular systems. Biophys Rev 2018; 10:317-26. [PMID: 29243093].

49. Sanz-Hernández M, Vostrikov VV, Veglia G, De Simone A. Accurate Determination of Conformational Transitions in Oligomeric Membrane Proteins. Sci Rep 2016; 6:23063-[PMID: 26975211].

50. Hawe A, Sutter M, Jiskoot W. Extrinsic Fluorescent Dyes as Tools for Protein Characterization. Pharm Res 2008; 25:1487-99. [PMID: 18172579].

51. Arosio P, Knowles TP, Linse S. On the lag phase in amyloid fibril formation. Phys Chem Chem Phys 2015; 17:7606-18. [PMID: 25719972].

52. Pease LF III, Sorci M, Guha S, Tsai D-H, Zachariah MR, Tarlov MJ, Belfort G. Probing the nucleus model for oligomer formation during insulin amyloid fibrillogenesis. Biophys J 2010; 99:3979-85. [PMID: 21156140].

53. Thakur AK, Jayaraman M, Mishra R, Thakur M, Chellgren VM, Byeon I-JL, Anjum DH, Kodali R, Creamer TP, Conway JF. Polyglutamine disruption of the huntingtin exon 1

N-terminus triggers a complex aggregation mechanism. Nat Struct Mol Biol 2009; 16:380-9. [PMID: 19270701].

54. Wei L, Jiang P, Xu W, Li H, Zhang H, Yan L, Chan-Park MB, Liu X-W, Tang K, Mu Y. The molecular basis of distinct aggregation pathways of islet amyloid polypeptide. J Biol Chem 2011; 286:6291-300. [PMID: 21148563].

55. Schafheimer N, Wang Z, Schey K, King J. Tyrosine/Cysteine cluster sensitizing human γD-crystallin to ultraviolet radiation-iunduced photoaggregation in vitro. Biochemistry 2014; 53:979-90. [PMID: 24410332].

56. Stefani M. Protein folding and misfolding on surfaces. Int J Mol Sci 2008; 9:2515-42. [PMID: 19330090].

57. Kaylor J, Bodner N, Edridge S, Yamin G, Hong D-P, Fink AL. Characterization of oligomeric intermediates in α-synuclein fibrillation: FRET studies of Y125W/Y133F/Y136F α-synuclein. J Mol Biol 2005; 353:357-72. [PMID: 16171820].

58. Olsen JV, Ong S-E, Mann M. Trypsin cleaves exclusively C-terminal to arginine and lysine residues. Mol Cell Proteomics 2004; 3:608-14. [PMID: 15034119].

59. Fontana A, de Laureto PP, Spolaore B, Frare E, Picotti P, Zambonin M. Probing protein structure by limited proteolysis. Acta Biochimica Polonica-English Edition 2004;51:299–322.

60. Frare E, Mossuto MF, de Laureto PP, Tolin S, Menzer L, Dumoulin M, Dobson CM, Fontana A. Characterization of oligomeric species on the aggregation pathway of human lysozyme. J Mol Biol 2009; 387:17-27. [PMID: 19361437].

61. Walker JM. The bicinchoninic acid (BCA) assay for protein quantitation, The protein protocols handbook. Springer 2009;11–15.

62. Susi H, Byler DM. Resolution-enhanced fourier transform infrared spectroscopy of enzymes. Methods Enzymol 1986; 130:290-311. [PMID: 3773736].

Articles are provided courtesy of Emory University and the Zhongshan Ophthalmic Center, Sun Yat-sen University, P.R. China. The print version of this article was created on 1 July 2021. This reflects all typographical corrections and errata to the article through that date. Details of any changes may be found in the online version of the article.